RSC Advances

PAPER

View Article Online
View Journal | View Issue

Cite this: RSC Adv., 2016, 6, 103700

Cu_2O hollow structures—microstructural evolution and photocatalytic properties†

Baoshun Wang,[a] Weiwei Zhang,[b] Zhiyun Zhang,[a] Renying Li,[a] Yulong Wu,[a] Zhengguang Hu,[a] Xiaoling Wu,[a] Chungang Guo,[a] Guoan Cheng[a] and Ruiting Zheng*[a]

Received 8th September 2016
Accepted 6th October 2016

DOI: 10.1039/c6ra22474a

www.rsc.org/advances

In this paper, Cu_2O Single-Shelled Hollow (SSH) sub-micron spheres, Multi-Shelled Hollow (MSH) sub-micron spheres and Multi-Shelled Porous (MSP) sub-micron spheres were successfully synthesized *via* a facile one-pot route in the presence of hexadecyltrimethylammonium bromide (CTAB) and ascorbic acid (VC). It is found that the morphology and structure of Cu_2O hollow nanoparticles can be adjusted by changing alkalinity and aging time. The formation mechanism and structural evolution for these hollow structures is studied. Among three kinds of Cu_2O hollow spheres, the Cu_2O MSH sub-micron spheres demonstrated the best photo-catalytic (PC) property, which should attribute to the higher light absorption and smaller band gap.

1. Introduction

In recent years, hollow micro-/nanostructures aroused a lot of interest because of their unique properties such as low density, high specific surface area and efficient paths for ion diffusion, which make them have potential applications in energy storage, catalysts, sensors, drug-delivery carriers, photonic crystals, biomedical diagnosis agents, chemical reactors and so on.[1–10] In previous researches, different strategies, such as the Kirkendall effect,[3,6] template-mediated approaches,[11,12] Ostwald ripening,[13,14] galvanic replacement,[15,16] chemical etching,[17–28] water-soluble salt templates have been developed to synthesize hollow structures.[19,20]

As a typical p-type semiconductor, cuprous oxide (Cu_2O) has been widely applied in catalysis,[21] gas sensors,[22] biosensing,[23] solar cells,[24] photoelectrochemical cells,[25] and lithium-ion batteries.[26] Lots of progresses have been made in synthesizing different shape of Cu_2O hollow structures. Lu and co-workers synthesized octahedral Cu_2O hollow nanocages *via* a catalytic self-templating method.[27] Zeng and co-workers firstly synthesized colloidal CuO nanocrystallites, then CuO spherical aggregation and transformed into hollow Cu_2O nanospheres.[28] Xu *et al.*[29] report the synthesis of multi-shelled hollow Cu_2O spheres by the help of vesicle templates. Multi-shelled hollow micro-/nanostructured materials are expected to have better performances over their single-shelled counterparts for applications in catalysis and photocatalysis.[30] However, the forming mechanism and their photocatalysis properties of hollow Cu_2O spheres still need further investigation.

In this paper, Cu_2O MSH, MSP and SSH sub-micron spheres were successfully synthesized *via* a facile one-pot route in the presence of hexadecyltrimethylammonium bromide (CTAB) and ascorbic acid (VC). We found that CTAB and VC play an important role in the formation of Cu_2O hollow spheres. And the structure of Cu_2O hollow spheres can be adjusted by simply changing alkalinity and etching time. At last, we made Cu_2O PEC devices with three kinds of hollow particles. The experimental results indicate three kinds of Cu_2O hollow structures all have good response to light. The photocurrent of Cu_2O MSH sub-micron spheres device is higher than the other two. The reason should attribute to its slightly lower band gap and larger absorption range.

2. Experimental section

2.1. The chemicals

Copper(II) sulfate pentahydrate ($CuSO_4 \cdot 5H_2O$, 99%) was purchased from Xilong Chemical Co. Hexadecyltrimethylammonium bromide ($C_{19}H_{42}BrN$, 99%) and ascorbic acid ($C_6H_8O_6$, 99.7%) were purchased from Sinopharm Chemical Reagent Co. Sodium hydroxide (NaOH, 98%) was purchased from Beijing Chemical Works. DI water was made in our lab.

2.2. Synthesis of Cu_2O hollow micro-/nanostructures

Cu_2O MSH sub-micron spheres were synthesized by a liquid chemical reaction. In a typical procedure, 3.6436 g of CTAB and 0.05 g of $CuSO_4 \cdot 5H_2O$ were put in a beaker with 100 mL deionized water, followed by vigorously stirred to obtain solution A. Then 0.18 g of ascorbic acid was added into solution A, and the beaker was immersed in 60 °C of oil bath for 20 min

[a]Key Laboratory of Radiation Beam Technology and Materials Modification of Ministry of Education, College of Nuclear Science and Technology, Beijing Normal University, Beijing 100875, P. R. China. E-mail: rtzheng@bnu.edu.cn

[b]School of Science, Minzu University of China, Beijing 10081, PR China

† Electronic supplementary information (ESI) available. See DOI: 10.1039/c6ra22474a

with the speed of 10 rpm to get solution B. After that, 10 mL 0.4 M of NaOH solution was added into above solution B drop by drop under the same rotate speed. The color of the solution B changes from blue to yellow immediately. The solution was stirred for 5 s, and then the precipitate was centrifuged, washed sequentially by de-ionized water and isopropyl alcohol for three times, respectively. After dried in a 60 °C vacuum oven for 5 h, the Cu_2O multi-shelled hollow spheres were obtained.

Using the similar procedure of Cu_2O MSH sub-micron spheres, just prolong reaction time to 10 min or increase the concentration of NaOH to 0.5 M (reaction time is 5 min). The products turn to be Cu_2O MSP sub-micron spheres. If we prolong reaction time to 1 h or increase the concentration of NaOH to 2.5 M (reaction time is 5 min). The products turn to be Cu_2O SSH sub-micron spheres.

2.3. Structural characterization

The chemical structure and components of as-prepared Cu_2O hollow sub-micron spheres were identified by X-ray diffraction (XRD, Bruker D8 Advance diffractometer) with Cu Kα radiation ($\lambda = 0.1506$ nm). Morphology and size of the as-prepared Cu_2O hollow sub-micron spheres were observed by scanning electron microscopy (SEM, HITACHI S-4800). Transmission electron microscopy (TEM) and high-resolution TEM (HRTEM) images were obtained by a F20 transmission electron microscopy. Room temperature UV-vis diffuse reflectance spectra were taken on a PerkinElmer Lambda 950 UV-vis spectrophotometer.

2.4. Photocurrent measurements

20 mg of as-prepared Cu_2O powder was dispersed in 15 mL de-ionized water to make a stable suspension. Then two drops of suspension was dropped onto a piece of FTO glass and dried in a 60 °C thermostat for slowly drying. Copper wires were used to contact the dried thin films. The areas of thin film electrodes were about 1 cm^2. Photocurrent measurements were carried out on a bipotentiostat (Modle AFCBP1, USA) in the darkness. The light source employed in PEC activity was a 300 W xenon lamp with an AM 1.5G filter (MAX-302, Asahi Spectra, USA). For all the measurements, three-electrode system was applied, as Fig. S1 shows (see ESI†). The electrolyte was 0.5 M Na_2SO_4 electrolyte solution (pH = 7) deaerated by bubbling N_2 for at least 25 min before each experiment. A platinum line was used as a counter electrode, and Ag/AgCl (in 3.0 M KCl solution) was used as a reference electrode connected to Na_2SO_4 solution by a salt bridge. Photocurrent measurements were taken from 0 to −1 V *vs.* Ag/AgCl at a scan rate of 5 mV s^{-1}. All potentials reported in this study are relative to Ag/AgCl (3 M KCl, 0.207 V *vs.* SHE).

3. Results and discussion

3.1. Microstructure of hollow structures

Fig. 1 shows the structures of the three as-prepared products. It can be seen that three kinds of as-prepared products are all sub-micron hollow spheres, but their microstructure are different. Fig. 1(a) is the TEM image of a MSH sphere. It can be observed that the sphere has three layers, the thickness of each layer is about 10 nm. Fig. 1(d) is the SEM image of MSH spheres. The MSH spheres are all closed spheres, the average diameter of spheres is about 150 nm. While we keep other conditions unchanged, just prolong the reaction time to 10 minutes, MSP spheres can be obtained. Fig. 1(b) clearly shows the structure of MSP spheres, we can found that these porous spheres have a multi-shelled structure and the average shell thickness is about 22.55 nm. Fig. 1(e) is the SEM image of MSP spheres. The average diameter of porous sub-micron sphere is about 150–200 nm and the average diameter of the pores on the sphere surface is about 30 nm. As the reaction time further extended to 1 hour, MSP spheres turn into SSH spheres, as shown in

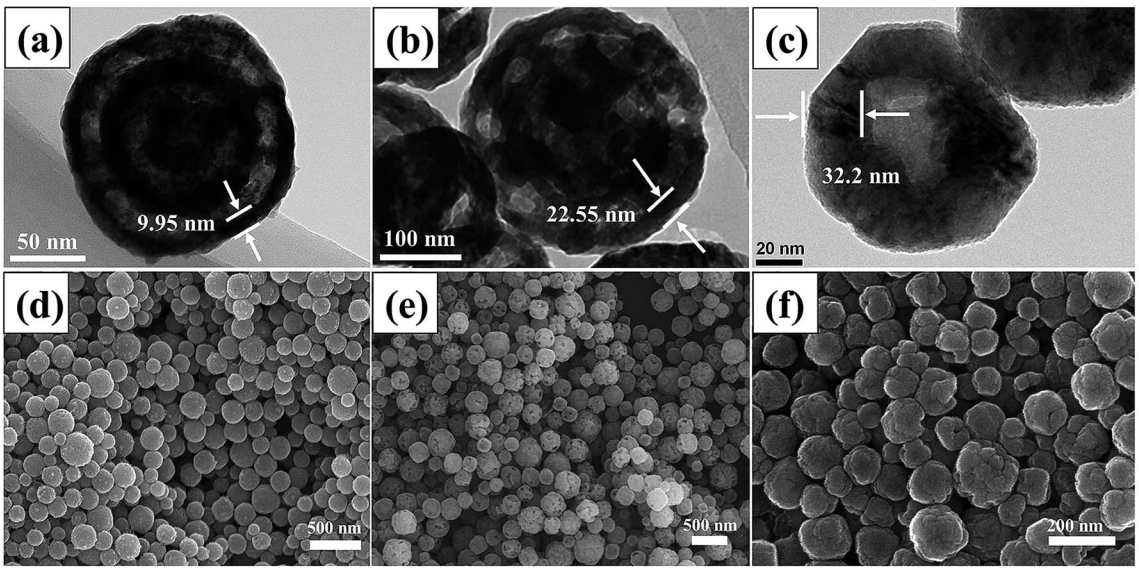

Fig. 1 TEM and SEM images of three kinds of Cu_2O hollow structures. (a) TEM image of MSH spheres, (b) TEM image of MSP spheres, (c) TEM image of SSH spheres, (d) SEM image of MSH spheres, (e) SEM images of MSP spheres, (f) SEM image of SSH spheres.

Fig. 1(c). TEM image shows that these particles have an obvious empty interior. The average shell thickness of the hollow sphere is about 32.2 nm. SEM image (Fig. 1(f)) indicates that some of the particles have a pore on their surface. The average diameter of hollow sphere is still 150–200 nm.

Fig. 2 shows the typical XRD pattern of the as-prepared MSH, MSP and SSH sub-micron spheres. All the XRD patterns contain five distinguishable and broadened diffraction peaks at 29.63°, 36.50°, 42.40°, 61.52°, 73.70°, 77.57°, respectively. The peaks can be perfectly indexed to (110), (111), (200), (220), (311) and (222) lattice planes of cubic Cu_2O (JCPDS file no. 65-3288). The XRD pattern of MSP and SSH spheres also contain other weak CuO peaks at 35.50°, 38.73°, 48.73°, respectively. *i.e.* (002), (111), (202) lattice planes of monoclinic CuO (JCPDS file no. 48-1548) which means CuO was formed with the increase of reaction time. But the main component of MSPS and SSHS is still Cu_2O.

3.2. Formation mechanism of multi-shelled Cu_2O spheres

Some researchers studied the formation mechanism of multi-shelled Cu_2O spheres. Xu *et al.*[29] pointed out that CTAB plays a vital template-mediated role in the formation of different Cu_2O hollow architecture. However, Qi *et al.*[31] found that Xu's method is hard to extend to other materials due to the unstable structure of vesicle templates and their high sensitivity on reaction environments. In previous researches, VC usually was thought as reducing agent. We found that except CTAB, VC also works as a part of template in the synthesis of Cu_2O hollow structure. Three experiments were carried out to testify our assumption. The results are shown in Fig. 3. If we use glucose with the same mole number as a reducing agent, after adding NaOH solution, the color of the solution changed from blue to white-blue. After three minutes of reaction, the solution turns to be yellow. The reaction product is solid Cu_2O octahedron rather than sphere, as shown in Fig. 3(a). If we used hydrazine with the same mole number as a reducing agent, the color of the solution turned from blue to yellow immediately after we added the hydrazine into Cu_2SO_4 solutions. In this reaction, solid Cu_2O spheres with some small particles attached on them were formed, as shown in Fig. 3(b). The reducibility of VC is stronger than glucose but weaker than hydrazine. None of hollow structure was obtained by other two reducing agents. Meanwhile, if we change the adding order of VC and NaOH in the experiment. It could be found that Cu_2O dodecahedron rather than sphere was obtained, as shown in Fig. 3(c). So we conjecture that except working as reducing agent, VC also works as a supplementary template in the formation of different Cu_2O hollow spheres.

The formation mechanism of Cu_2O hollow structure is shown in Fig. 4. In the initial stages of the reaction, CTAB is easy to form micelles and closed bilayer aggregates such as vesicles under the assist of VC, as shown in step I of Fig. 4. When $CuSO_4$ solution is injected into the solution Cu^{2+} ions will be absorbs on the surface of CTAB vesicles. After a while, Cu^{2+} ions was uniformly distributed in the vesicle shell, as shown in step II of Fig. 4. When NaOH was added in the solution, multi-shelled $Cu(OH)_2$ spheres were formed immediately and be simultaneously reduced into Cu_2O by VC, as shown in step III of Fig. 4. The formation process of multi-shelled hollow Cu_2O spheres can be described by reaction eqn (1) and (2).

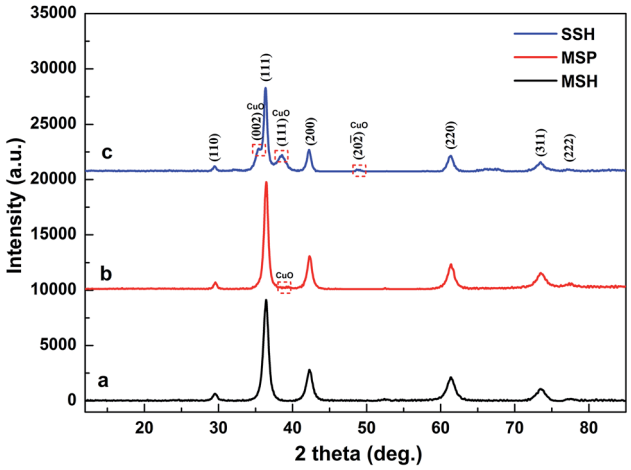

Fig. 2 Powder XRD pattern of different products. (a) MSH spheres, (b) MSP spheres, (c) SSH spheres.

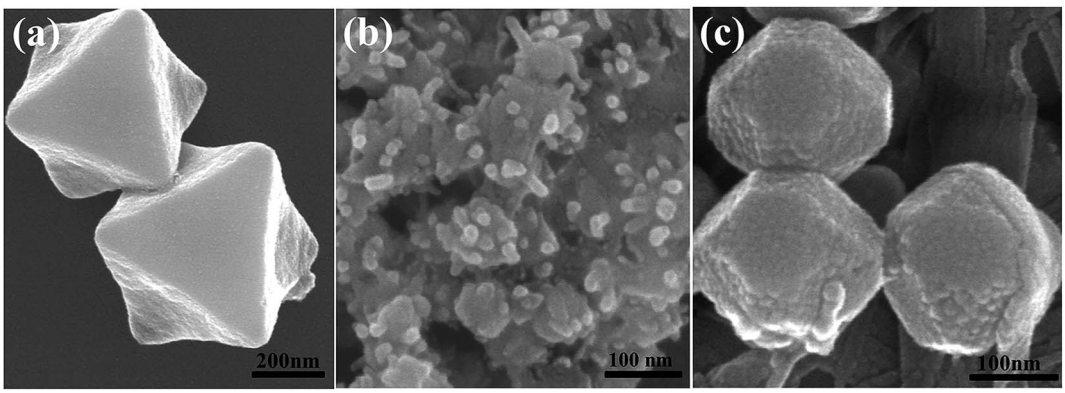

Fig. 3 SEM images of products obtained by different chemical reactions. (a) Using glucose as the reductant, (b) using hydrazine as the reductant, (c) change the adding order of VC and NaOH.

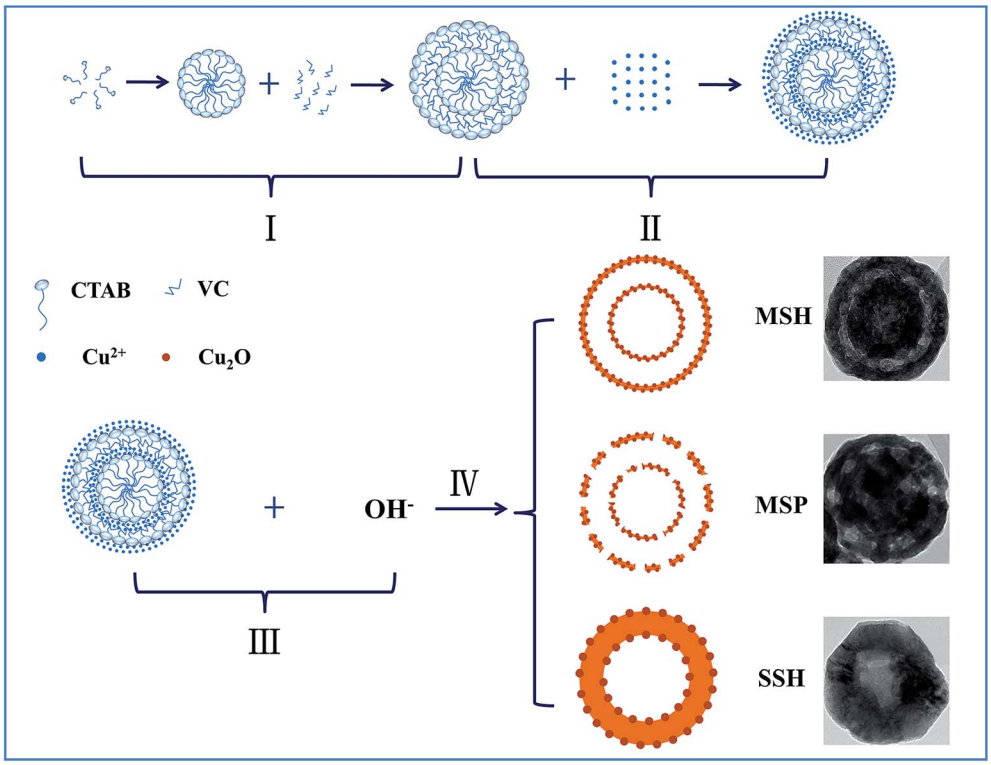

Fig. 4 Schematic illustration of the formation mechanism of Cu_2O MSH, MSP and SSH: (I) sphere template micelle molecule was formed by CTAB vesicles under the assist of VC. (II) Cu^{2+} absorbed on the surface of CTAB vesicles. (III) When NaOH was added in the solution, multi-shelled $Cu(OH)_2$ hollow spheres were formed immediately and simultaneously reduced into Cu_2O by VC. (IV) When the reaction time was 5 seconds, 10 minutes and 1 hour can form MSH, MSP and SSH, respectively.

$$Cu^{2+} + 2OH^- \rightarrow Cu(OH)_2\downarrow \quad (1)$$

$$2Cu(OH)_2 + C_6H_8O_6 \rightarrow Cu_2O\downarrow + C_6H_6O_6 + 3H_2O \quad (2)$$

From above experiments, we can find that CTAB vesicles are unstable in alkaline solution. Using glucose as a reducing agent, reducing rate of $Cu(OH)_2$ is slowly. Moreover, the CTAB vesicle is damaged in the alkaline solution. When the Cu_2O nano particles are formed in the solution, they tend to attach on the existing Cu_2O particles and forms Cu_2O octahedrons by orientation growth. When we change the adding order of VC and NaOH, CTAB vesicles are destroyed firstly. Similarly, Cu_2O tend to orientation growth, we just obtain Cu_2O dodecahedrons. Hydrazine is an alkaline reducing agent and the reducing rate of hydrazine is much faster than glucose and VC, when the hydrazine is adding into $CuSO_4$ solution, lots of Cu_2O nano particles are formed at the same time. These particles will aggregate and forms solid Cu_2O spheres. During the course, CTAB vesicles are destroyed, because we do not find any hollow structure in the product.

3.3. Microstructure evolution of Cu_2O spheres in alkali solutions

On the basis of the above analysis, the formation process and mechanism of multi-shelled Cu_2O hollow structures could be illustrated by Fig. 4. But the structure evolution of Cu_2O hollow structures is not well understood.

A time-dependent experiment was carried out to investigate the structural evolution of Cu_2O hollow structure. Using the typical synthesis procedure, the samples obtained at various reaction times were inspected by TEM, as shown in Fig. 5(a)–(f). We found that MSH sub-micron spheres can be synthesized after five seconds of reaction (Fig. 5(a)). After 3 minutes of reaction, MSH and MSP sub-micron spheres can be observed in the product (Fig. 5(c)). When we prolong the reaction time to 10 min, MSH sub-micron spheres completely transformed into MSP sub-micron spheres. If the reaction time was further increased to 30 minutes, some SSH sub-micron spheres were observed in the product (Fig. 5(e)). After 60 minutes' reaction, all the products are SSH sub-micron spheres, as shown in Fig. 5(f). The structural evolution of Cu_2O hollow structures is illustrated in step III of Fig. 4. Though the average size of Cu_2O hollow structure changes little, we can find that the shell thickness of the particles increases with the increase of reaction time. The reaction equation of the Cu_2O in alkaline solution could be described as follows:[32]

$$Cu_2O + OH^- + H_2O \rightarrow [Cu(OH)_2]^- + CuOH \quad (3)$$

$$2CuOH \rightarrow Cu_2O + H_2O \quad (4)$$

$$4CuOH + O_2 \rightarrow 4CuO + 2H_2O \quad (5)$$

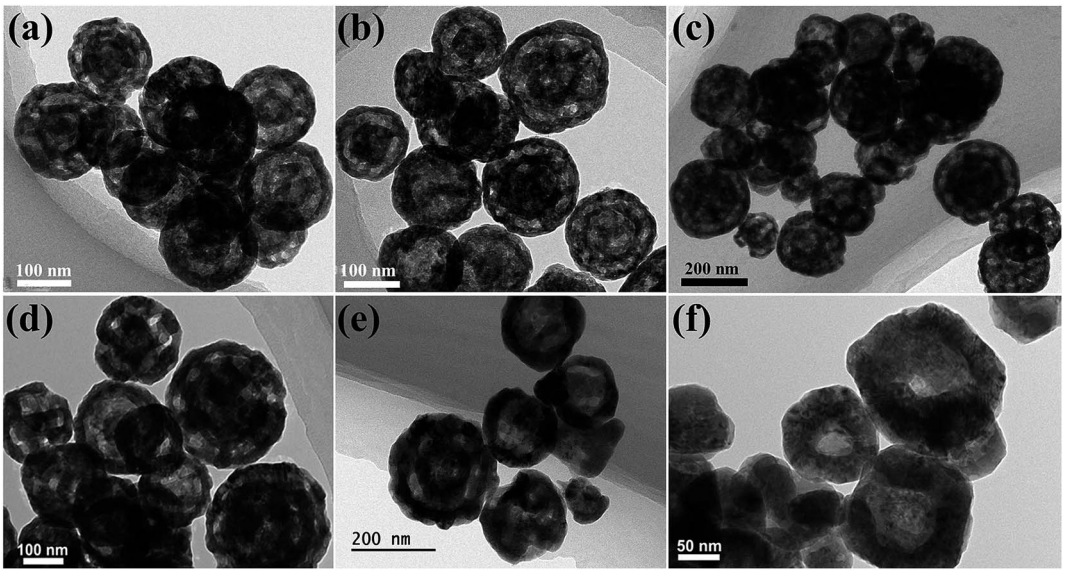

Fig. 5 TEM images of Cu_2O hollow structures obtained at various reaction times: (a) 5 s, (b) 30 s, (c) 3 min, (d) 10 min, (e) 30 min, (f) 1 h.

In alkaline solution, Cu_2O could reaction with OH^- and forms $[Cu(OH)_2]^-$ and CuOH. $[Cu(OH)_2]^-$ dissolves in water, CuOH is not stable, it's easy to decompose and forms Cu_2O or CuO (when O_2 exist). In this course, the pH value of the solution decrease gradually, which is consistent with our measurement of the pH in the solution, as shown in Fig. S2 (see ESI†). Moreover, when OH^- etch the surface and interior of Cu_2O MSH sub-micron spheres, Cu_2O continue to dissolve, which will form holes on the MSH sub-micron spheres and result in MSP sub-micron spheres. Due to the dissolution and precipitation of Cu_2O, Ostwald ripening happened. The new generated Cu_2O would deposit on the interior surface to increase the thickness of the shell. The formation process of MSHS can be described by reaction eqn (3) and (4). Since the inner smaller particles have a higher specific surface area, so the dissolution rate of inner particles is relatively fast than the external surface. Ostwald ripening and surface reconstruction will make multi-shelled hollow structure transform into single-shelled hollow structures in the following 1 hour. Meanwhile, because there is some O_2 in the solution, reaction eqn (5) would happen and CuO will form. These phenomenon can be verified by the XRD pattern (Fig. 2). If we increase the mole number of NaOH to 2.5 M, the Cu_2O multi-shelled hollow structure will transform into single-shelled hollow structures in 10 minutes, as Fig. S3 shows (see ESI†).

3.4. Relationship between microstructure and photoelectrochemical response

Fig. 6 is the photoelectrochemical response of Cu_2O different hollow micro-/nanostructures in 0.5 M Na_2SO_4 solution under 300 W Xe lamp (intensity: 100 mW cm^{-2}) with 5 s light on/off cycles through AM 1.5G optical filter illumination. This photo-induced cathodic current results from the reduction of protons involving the photo-generation of electrons, and reveals the p-type nature of the Cu_2O photoelectrode.[33] It also reveal the interfacial generation and separation dynamics of photogenerated charges of semiconductor photocatalysts. A larger photocurrent indicates higher electrons and holes separation efficiency.[34] The results indicate that three Cu_2O hollow spheres obtained in this paper have strong response to the sun light. The photocurrent values of MSH, MSP and SSH sub-micron sphere films at −0.45 V *versus* Ag/AgCl are about 0.08 mA cm^{-2}, 0.06 mA cm^{-2}, 0.07 mA cm^{-2}, respectively. The MSH sub-micron spheres have highest photocurrent than the other two materials.

The photocurrent values indicate that MSH sub-micron spheres has the best photoelectrochemical response, but the reason is not clear. The ultraviolet-visible reflectance spectra experiment was carried out to study the corresponding band gaps of three samples.

Fig. 7(a) shows the ultraviolet-visible diffuse reflectance spectra of three samples. The corresponding band gaps were

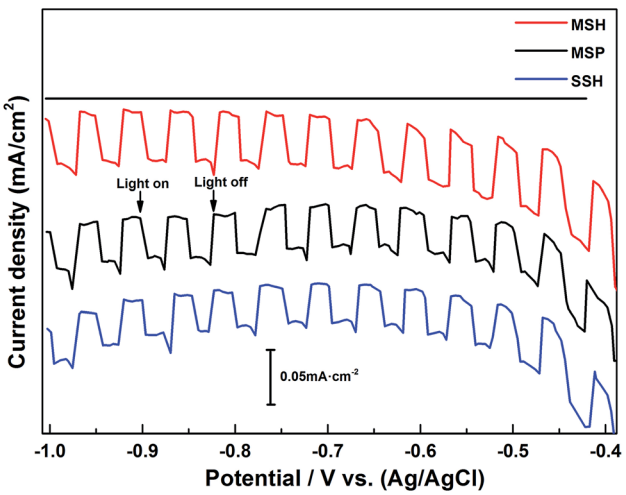

Fig. 6 Current density–potential responses of different Cu_2O hollow micro-/nanostructures in 0.5 M Na_2SO_4 solution under 300 W Xe lamp through AM 1.5 optical filter illumination.

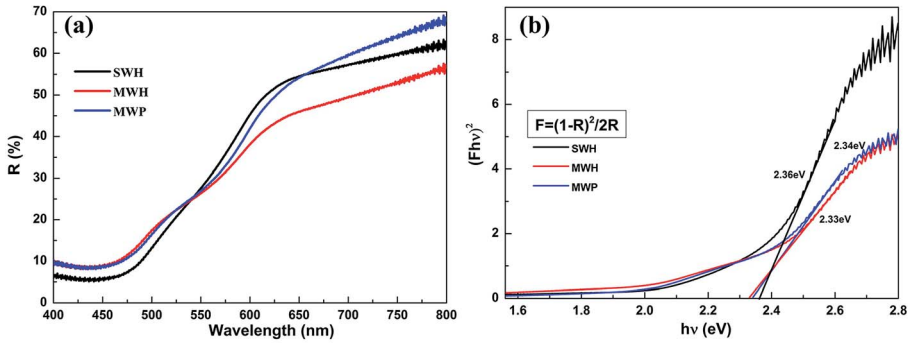

Fig. 7 (a) Ultraviolet-visible diffuse reflectance spectra of MSH, MSP and SSH sub-micron spheres. (b) $(Fh\nu)^2$ as a function of photon energy ($h\nu$), where F is the Kubelka–Munk function of the diffuse reflectance R from (a). The intercepts of extrapolated straight lines give the corresponding direct bandgaps of different Cu_2O hollow structures.

obtained from the corresponding modified Kubelka–Munk function,[35] as shown in Fig. 7(b). The band gap of MSH, MSP and SSH sub-micron spheres are 2.33 eV, 2.36 eV, and 2.34 eV, respectively. It can be seen that MSH sub-micron spheres have a slightly lower band gap than SSH and MSP sub-micron spheres, which is in agreement with its lower reflectance in Fig. 7(a). That is to say, MSH sub-micron spheres have larger absorption range and could harvest more solar energy to generate more electron–hole pairs to join in the redox reaction on the surface, which will produce bigger photocurrent.

4. Conclusion

In summary, in this paper Cu_2O single-shelled hollow spheres, multi-shelled hollow spheres and multi-shelled porous spheres were successfully synthesized *via* a facile and one-pot route in the presence of hexadecyltrimethylammonium bromide (CTAB) and ascorbic acid (VC). The morphology and structure of Cu_2O nanoparticles can be adjusted by changing alkalinity and duration. CTAB and VC work as a template-mediated and OH^- work as an etching agent in the formation of different hollow structures. The obtained different morphologies Cu_2O hollow spheres were active photocatalysts for solar water-splitting. The results indicate that these special morphologies Cu_2O hollow spheres have strong response under the simulated sunlight (the AM 1.5 spectrum) illumination. The Cu_2O multi-shelled hollow spheres demonstrated an enhanced photocatalytic. Further investigation indicates that the difference of PEC efficiency should attribute to the Cu_2O MSH sub-micron spheres have smaller band gap and larger light absorption.

Acknowledgements

This work is supported by the National Nature Science Foundation of China (11575025) and the Fundamental Research Funds for the Central Universities.

References

1 A. D. Dinsmore, M. F. Hsu, M. G. Nikolaides, M. Marquez, A. R. Bausch and D. A. Weitz, *Science*, 2002, **298**, 1006.
2 Y. G. Sun and Y. N. Xia, *Science*, 2002, **298**, 2176.
3 Y. Yin, R. M. Rioux, C. K. Erdonmez, S. Hughes, G. A. Somorjai and A. P. Alivisatos, *Science*, 2004, **304**, 711.
4 H. G. Yang and H. C. Zeng, *Angew. Chem., Int. Ed.*, 2004, **43**, 5930.
5 J. F. Chen, H. M. Ding, J. X. Wang and L. Shao, *Biomaterials*, 2004, **25**, 723.
6 J. Yang, L. Qi, C. Lu, J. Ma and H. Cheng, *Angew. Chem., Int. Ed.*, 2005, **44**, 598.
7 J. Y. Chen, F. Saeki, B. J. Wiley, H. Cang, M. J. Cobb, Z. Y. Li, L. Au, H. Zhang, M. B. Kimmey, X. D. Li and Y. N. Xia, *Nano Lett.*, 2005, **5**, 473.
8 X. W. Lou and L. A. Archer, *Adv. Mater.*, 2008, **20**, 1853.
9 Q. H. Cui, Y. S. Zhao and J. N. Yao, *J. Mater. Chem.*, 2012, **22**, 4136.
10 N. Venugopal, D. J. Lee, Y. J. Lee and Y. K. Sun, *J. Mater. Chem. A*, 2013, **1**, 13164.
11 K. J. C. van Bommel, A. Friggeri and S. Shinkai, *Angew. Chem., Int. Ed.*, 2003, **42**, 980.
12 X. W. Lou, L. A. Archer and Z. Yang, *Adv. Mater.*, 2008, **20**, 3987.
13 H. G. Yang and H. C. Zeng, *Angew. Chem., Int. Ed.*, 2004, **43**, 5206.
14 H. C. Zeng, *J. Mater. Chem. A*, 2011, **21**, 7511.
15 Y. Sun, B. Mayers and Y. Xia, *Adv. Mater.*, 2003, **15**, 641.
16 K. An and T. Hyeon, *Nano Today*, 2009, **4**, 359.
17 Q. Zhang, T. Zhang, J. Ge and Y. Yin, *Nano Lett.*, 2008, **8**, 2867.
18 K. Y. Niu, J. Yang, S. A. Kulinich, J. Sun, H. Li and X. W. Du, *J. Am. Chem. Soc.*, 2010, **132**, 9814.
19 X. W. Lou, C. Yuan, Q. Zhang and L. A. Archer, *Angew. Chem., Int. Ed.*, 2006, **45**, 3825.
20 M. R. Kim and D. J. Jang, *Chem. Commun.*, 2008, **41**, 5218.
21 H. L. Xu, W. Z. Wang and W. Zhu, *J. Phys. Chem. B*, 2006, **110**, 13829.
22 H. G. Zhang, Q. S. Zhu, Y. Zhang, Y. Wang, L. Zhao and B. Yu, *Adv. Funct. Mater.*, 2007, **17**, 2766.
23 X. Li, H. Gao, C. J. Murphy and L. Gou, *Nano Lett.*, 2004, **4**, 1903.
24 M. Diab, B. Moshofsky, I. J. Plante and T. Mokari, *J. Mater. Chem.*, 2011, **21**, 11626.

25 W. Z. Wang, X. W. Huang, S. Wu, Y. X. Zhou, L. J. Wang, H. L. Shi, Y. J. Liang and B. Zou, *Appl. Catal., B*, 2013, **134**, 293.
26 Y. Yao, M. T. McDowell, I. Ryu, H. Wu, N. Liu, L. B. Hu, W. D. Nix and Y. Cui, *Nano Lett.*, 2011, **11**, 2949.
27 C. H. Lu, L. M. Qi, J. H. Yang, X. Y. Wang, D. Y. Zhang, J. L. Xie and J. M. Ma, *Adv. Mater.*, 2005, **17**, 2562.
28 Y. Chang, J. J. Teo and H. C. Zeng, *Langmuir*, 2005, **21**, 1074.
29 H. L. Xu and W. Z. Wang, *Angew. Chem.*, 2007, **46**, 1489.
30 J. Y. Wang, H. J. Tang, L. J. Zhang, H. Ren, R. B. Yu, Q. Jin, J. Qi, D. Mao, M. Yang, Y. Wang, P. R. Liu, Y. Zhang, Y. R. Wen, L. Gu, G. H. Ma, Z. G. Su, Z. Y. Tang, H. J. Zhao and D. Wang, *Nature Energy*, 2016, **1**, 1.
31 J. Qi, X. Y. Lai, J. Y. Wang, H. J. Tang, H. Ren, Y. Yang, Q. Jin, L. J. Zhang, R. B. Yu, G. H. Ma, Z. G. Su, H. J. Zhao and D. Wang, *Chem. Soc. Rev.*, 2015, **44**, 6749.
32 A. A. Aref, L. B. Xiong, N. N. Yan, A. M. Abdulkarem and Y. Yu, *Mater. Chem. Phys.*, 2011, **127**, 433.
33 Y. K. Hsua, C. H. Yua, Y. C. Chen and Y. G. Lin, *Electrochim. Acta*, 2013, **105**, 62.
34 Y. M. He, J. Cai, T. T. Li, Y. Wu, H. J. Lin, L. H. Zhao and M. F. Luo, *Chem. Eng. J.*, 2013, **215**, 721.
35 T. J. McCarthy, T. A. Tamer and M. G. Kanatzidis, *J. Am. Chem. Soc.*, 1995, **117**, 1294.